Desalination and Water Treatment
www.deswater.com
doi: 10.1080/19443994.2015.1030708

57 (2016) 9307–9317
April

Taylor & Francis
Taylor & Francis Group

Adsorption of Victoria Blue R (VBR) dye on magnetic microparticles containing Fe(II)–Co(II) double salt

Kadir Erol[a], Kazım Köse[b], Dursun Ali Köse[a], Ümit Sızır[a], İlknur Tosun Satır[a], Lokman Uzun[c,*]

[a]*Faculty of Science and Literature, Department of Chemistry, Hitit University, Çorum, Turkey, Tel. +90 364 227 70 00, ext. 1711; email: kadirerol86@gmail.com (K. Erol), Tel. +90 364 227 70 00, ext. 1635; email: dkose@hacettepe.edu.tr (D.A. Köse), Tel. +90 542 428 5984; email: umit_sizir@hotmail.com (Ü. Sızır), Tel. +90 364 227 7000, ext. 1642; email: ilknurtosun@hitit.edu.tr (İ. Tosun Satır)*
[b]*Scientific Technical Research and Application Center, Hitit University, Çorum, Turkey, Tel. +90 364 219 2866; email: kazim8080@gmail.com*
[c]*Faculty of Science, Department of Chemistry, Hacettepe University, 06381-Beytepe, Ankara, Turkey, Tel. +90 312 297 7337; Fax: +90 312 299 2163; email: lokman@hacettepe.edu.tr*

Received 15 September 2014; Accepted 9 March 2015

ABSTRACT

Magnetic microparticles have many applications in various areas today. The aim of this study was to develop hydrophobic magnetic microparticles as an alternative to traditional methods for high capacity and low cost removal of Victoria Blue R (VBR), which is valuable for industry and commercial, from wastewater and to determine the VBR adsorption ability of this adsorbent. Fe(II)–Co(II) double salt incorporated magnetic poly(2-hydroxyethyl methacrylate-N-methacryloyl-L-tryptophan) [m-poly(HEMA-MATrp)] microparticles were synthesized and used as adsorbent. These microparticles were synthesized in aqueous dispersion medium via microemulsion polymerization using MATrp and HEMA monomers. Magnetic hydrophobic microparticles were characterized via Fourier transform infrared spectroscopy, scanning electron microscopy, and vibrating sample magnetometer. Adsorption experiments were conducted for different conditions (pH, interaction time, amount of microparticles, temperature, and ionic strength) in batch system. VBR adsorption capacity of magnetic hydrophobic microparticles was estimated as 89.46 μmol/g. Adsorption–desorption cycles were repeated 4 times, and there was no significant decrease for the adsorption capacity observed.

Keywords: Magnetic microparticle; Victoria Blue R; N-methacryloyl-L-tryptophan; Hydrophobic; Adsorption

1. Introduction

Azo dyes are chemical compounds used for coloring textile products [1–3]. They are frequently used for the food, pharmaceutical, and cosmetic industries due to the coloring properties [4]. Victoria Blue R (VBR) dye is one of the preferred textile dyes and poses an important place in the triphenyl methane dye family (Fig. 1). Existence of triphenyl methane dye derivatives showing phototoxic effects by forming reactive oxygen species in textile industry wastewater even at

*Corresponding author.

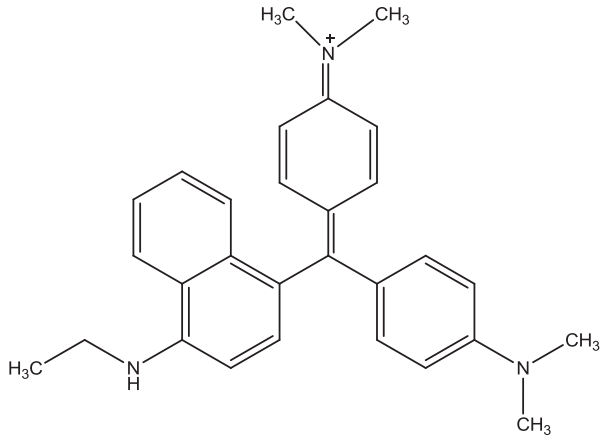

Fig. 1. Molecular structure of Victoria Blue R.

very low concentrations is an esthetically undesirable case as well as being a significant threat in terms of ecology [5–7]. Therefore, the process for color removal from the textile industry wastewater containing the dye color is of utmost importance. Nowadays, removal of dyes is carried out largely by physical and chemical methods. However, these methods are very expensive and disposal of the resulting large quantities of concentrated sludge causes problems. Therefore, alternative methods for protecting biological systems are needed to develop for the efficient removal of colorant from a large volume of wastewater effectively and affordably [8–10].

Most commonly used methods for wastewater treatment in textile industry are chemical oxidation methods, chemical precipitation and flocculation method, and purification by cucurbituril. Adsorption, membrane filtration, and ion exchange methods are physical, aerobic, anaerobic, and biosorption are biological methods used widely [11–17].

For recent years, applications of magnetic separation methods, in which small magnetic particles are used, and development of these methods are given great importance. Separation processes of biomaterials performed via usage of magnetic particles provide advantages in terms of application of biospecific affinity reactions, selectivity, simplicity, and speed [18–23]. All steps of the purification process of magnetic separation techniques can be carried out only a single sample container or in a test tube. Expensive chromatographic techniques or other equipment is not needed. Separation process may be carried out in crude samples containing directly suspended solid material. This feature of the magnetic adsorbents provides relatively easy and selective removal from the sample. In addition, the strength and effectiveness of magnetic separation process are very useful especially for large-scale systems [24–31].

In this study, the magnetic properties of the microparticles will be utilized via double salt produced via using nitrate salts of Fe(II)–Co(II) metals. Double salt synthesized was milled and incorporated into polymeric structure of poly(2-hydroxyethyl methacrylate-N-methacryloyl-L-tryptophan) [m-poly (HEMA-MATrp)]. The size of the monomers in the polymer to be formed is at the micrometer level, and it is envisaged that the existing polymeric structure will be used as an adsorbent for the removal of VBR from wastewater. By this method, it is intended that a much more effective method will be presented for the adsorption of textile dyes from wastewater in the literature. It is thought that a significant contribution will be provided for the removal of azo colorant from wastewater by combining the selectivity, simplicity, and speed of magnetic separation with separation techniques of the present.

2. Materials and methods

2.1. Chemicals

VBR (dye content 80%), toluene, sodium nitrite, potassium carbonate, iron(II) nitrate non-ahydrate, and cobalt(II) nitrate hexahydrate were obtained from Sigma-Aldrich (St. Louis, MO, USA). 2-Hydroxyethyl methacrylate (HEMA), ethylene glycol dimethacrylate (EGDMA), polyvinyl alcohol (PVA) (cold water soluble), L-tryptophan, and methacryloyl chloride were supplied from Aldrich (Munich, Germany). Azobisisobutyronitrile (AIBN) was obtained from Fluka (St. Gallen, Switzerland). N-methacryloyl-L-tryptophan (MATrp) was synthesized in laboratory conditions with respect to method considering literature [32]. All chemicals were of analytical grade and used as obtained.

2.2. Experimental methods

2.2.1. Synthesis of Fe(II)–Co(II) double salt

0.04 mol of $Fe(NO_3)_2{\cdot}9H_2O$ and $Co(NO_3)_2{\cdot}6H_2O$ were weighed and put in a beaker. Five hundred milliliters of distilled water was added on salts. Resultant solution was stirred magnetically at 50°C for 2 h. Water was removed via evaporator. The solid sample remained in the flask was dried in an oven at 110°C for 2 h. The dried sample was burned within crucible in oven at 900°C for 4 h and then crushed in a mortar.

2.2.2. Synthesis of microparticles containing Fe(II)–Co (II) double salt

Microemulsion polymerization technique was utilized for the synthesis of magnetic microparticles. Functional monomer 2-hydroxyethyl methacrylate (HEMA, 2 mL) and ethylene glycol dimethacrylate (EGDMA, 4 mL) were mixed, and 100 mg MATrp was added. Six milliliters of toluene was added after complete solution of MATrp, and monomer phase was achieved. Then, polyvinyl alcohol (PVA) of 200 mg was dissolved in 50 mL distilled water, and disperse phase was formed. The monomer phase and the disperse phase were mixed, and the mixture was treated with nitrogen gas (N_2) for 10 min. Fifty milligrams of AIBN and 1 g of Fe (II)–Co(II) magnetic double salt were mixed, and the mixture was stirred at the rate of 500 rpm at 65˚C for 6 h and just after at 650 rpm at 85˚C for 2 h. The magnetic microparticles obtained were washed extensively with ethanol and water by means of decantation processes. After completion of this step, microparticles were dried in a vacuum oven at 45–50˚C.

2.2.3. Characterization of microparticles

2.2.3.1. Analysis of magnetic properties. Magnetism degree of microparticles was determined via using vibrating sample magnetometer (VSM) (Quantum Design, Physical Properties Measurement System (PPMS), USA). Magnetism plot was obtained under the condition of external magnetic field of 20,000/+20,000 Gauss at room temperature. Magnetic properties of microparticles were obtained using hysteresis curve.

2.2.3.2. Surface morphology. The surface morphology magnetic microparticles were investigated by scanning electron microscopy (SEM; Carl Zeiss AG—EVO® 50 Series, Germany). Before investigation, sample was treated in freeze dryer to dry to be available for SEM analysis. Appropriate amount of sample was put on the sample holder plate and covered a thin gold layer under vacuum. As a last step, sample to be monitored via SEM was placed into the cell and images of sample were taken.

2.2.3.3. Fourier transform infrared spectroscopy analysis. Fourier transform infrared spectroscopy (FTIR) (Thermo Scientific, Nicolet IS10, USA) was used to determine characteristic functional groups of the magnetic microparticles. Magnetic microparticles, 2 mg dry, were obtained in form of pellets by mixing powder KBr (98 mg, IR-grade) homogeneously, and then, FTIR spectrum was obtained.

2.2.4. Adsorption studies

Batch system was preferred for adsorption experiments. Samples were prepared by mixing of 1.0 mL of VBR dye (100 mg/L) with 4.0 mL of buffer solution. Dye and buffer solution were equilibrated with mixing using rotator for 30 min. Then, adsorption was carried out by the addition of magnetic microparticles. Microparticles were precipitated at 9,000 rpm by centrifugation for 10 min after completion of adsorption. The quantification of dye molecules was performed by UV–vis spectrometry at 615 nm.

Adsorbed amount was calculated according to the following formula.

$$q = [(C_i - C_f) \times V]/m \quad (1)$$

wherein q is adsorbed amount (μmol/g), C_i (μmol/L) is the concentration of dye before adsorption, C_f (μmol/L) is the concentration of dye after adsorption, V (L) is the volume of adsorption media, and m (g) is the amount of magnetic microparticles.

2.2.5. Desorption and repeated use

Desorption of VBR dye which was adsorbed by magnetic microparticles was conducted batch wise. Dye-adsorbed particles (0.05 g) were stirred in 10 mL of desorption media containing 0.5 M HCI for 1 h continuously. To estimate the reusability of the particles, adsorption–desorption cycle was repeated four times using the same particle. Desorption ratio was calculated as follows:

$$\text{Desorption ratio } (\%) = [(\text{amount of dye desorbed})/(\text{total dye amount adsorbed})] \times 100$$

3. Results and discussion

3.1. Characterization of microparticles

3.1.1. Analysis of magnetic properties

Fig. 2 shows the curve of magnetism obtained via the VSM. The magnetic microparticles synthesized showed a typical hysteresis curve at room temperature and have a typical paramagnetic behavior. It was determined that saturation magnetism degree of magnetic polymer microparticles was less than that of bulk material. The cause for the loss of magnetism was that the oxidation during the process, and the presence of

oxidative initiators during process might lead the formation of some non-magnetic iron(II) oxide and cobalt(II) oxide.

3.1.2. Surface morphology

SEM images of the magnetic microparticles were given in Fig. 3. As shown, magnetic microparticles were in the shape of sphere and have rough surface characteristics. This roughness and porosity provide higher specific surface area and enhance adsorption ability of microparticles.

3.1.3. FT-IR analysis

Molecular formula and FT-IR spectrum of the magnetic microparticles were given in Figs. 4 and 5. As seen in the spectrum, the characteristics bands at 3,432 cm^{-1}, 2,956 cm^{-1}, 1,717 cm^{-1}, 1,643 cm^{-1}, and 1,456–1,381 cm^{-1} belong to CH alkyl stretching, C=O stretching, C=C stretching, OH stretching, and CN aromatic, respectively. These groups were included in functional monomer (MATrp) used. From these results, it could be said that functional monomer was incorporated successfully during polymerization process.

3.2. Adsorption experiments

3.2.1. Effect of pH

To investigate the effect of pH on adsorption capacity of magnetic microparticles, experiments were conducted at the pH interval of 3–11. The maximum adsorption capacity was achieved at pH 4.0 (Fig. 6). According to this result, charge distribution and hydrophobic interaction may closely be related with target dye molecule and functional monomer (MATrp). Indole ring in possession of VBR and

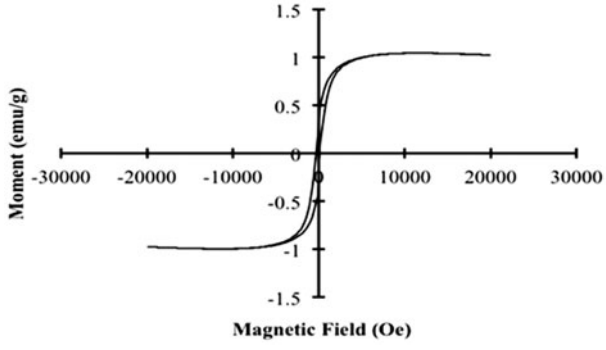

Fig. 2. Magnetism curve of microparticles.

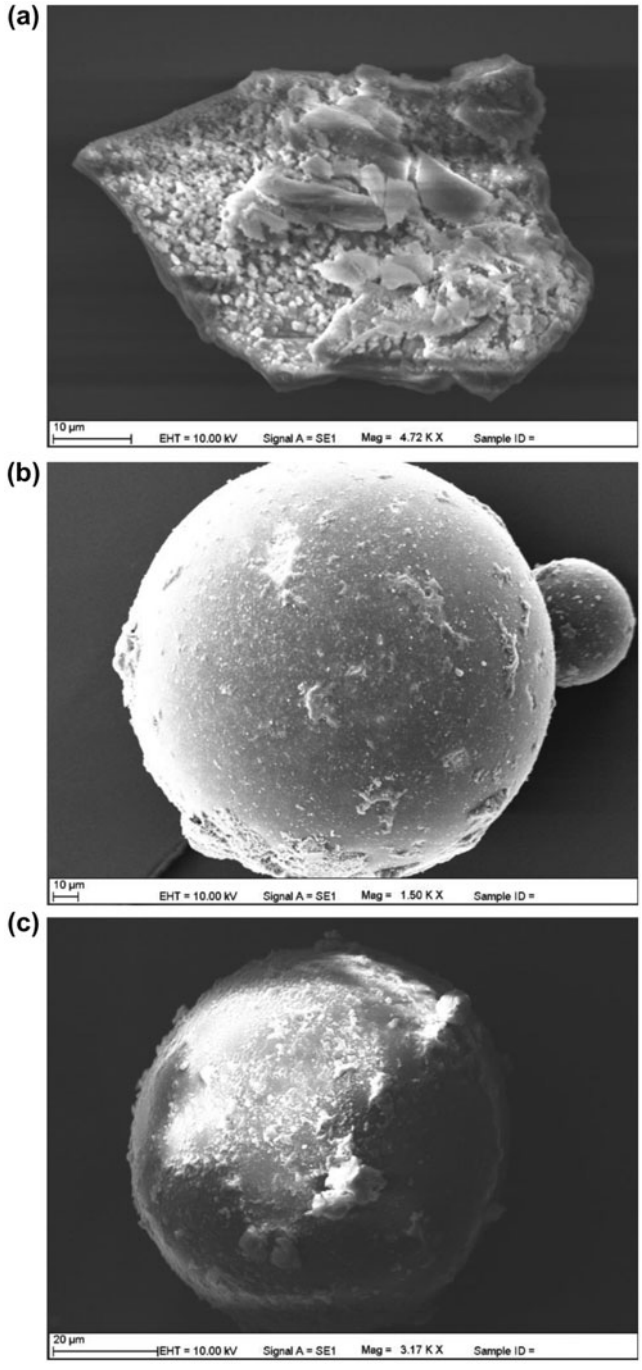

Fig. 3. SEM images of (a) magnetic Fe(II)–Co(II) double salt and (b and c) microparticles.

MATrp was almost uncharged (neutral) at pH 4.0. Because hydrophobic interactions are very effective when total net charge was zero, in this experiment, highest adsorption capacity was reached at pH 4.0 as well. Adsorption capacity was decreased at the higher and lower pH values due to the change of charge distribution at these pH values.

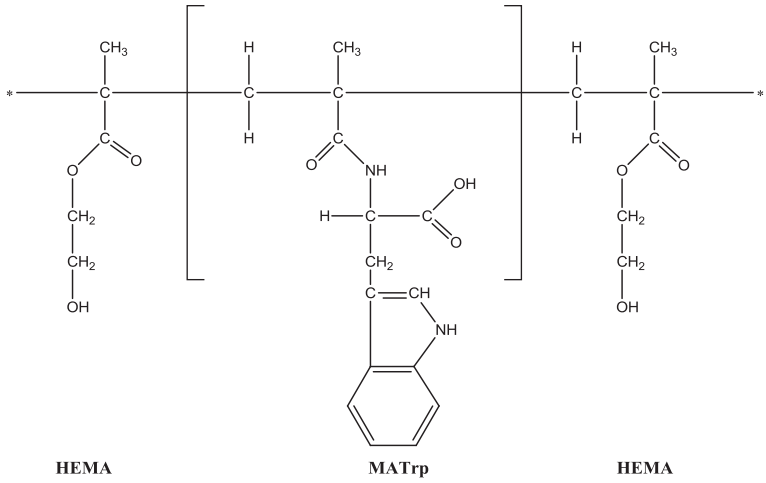

Fig. 4. Molecular structure of poly(HEMA-MATrp) microparticles.

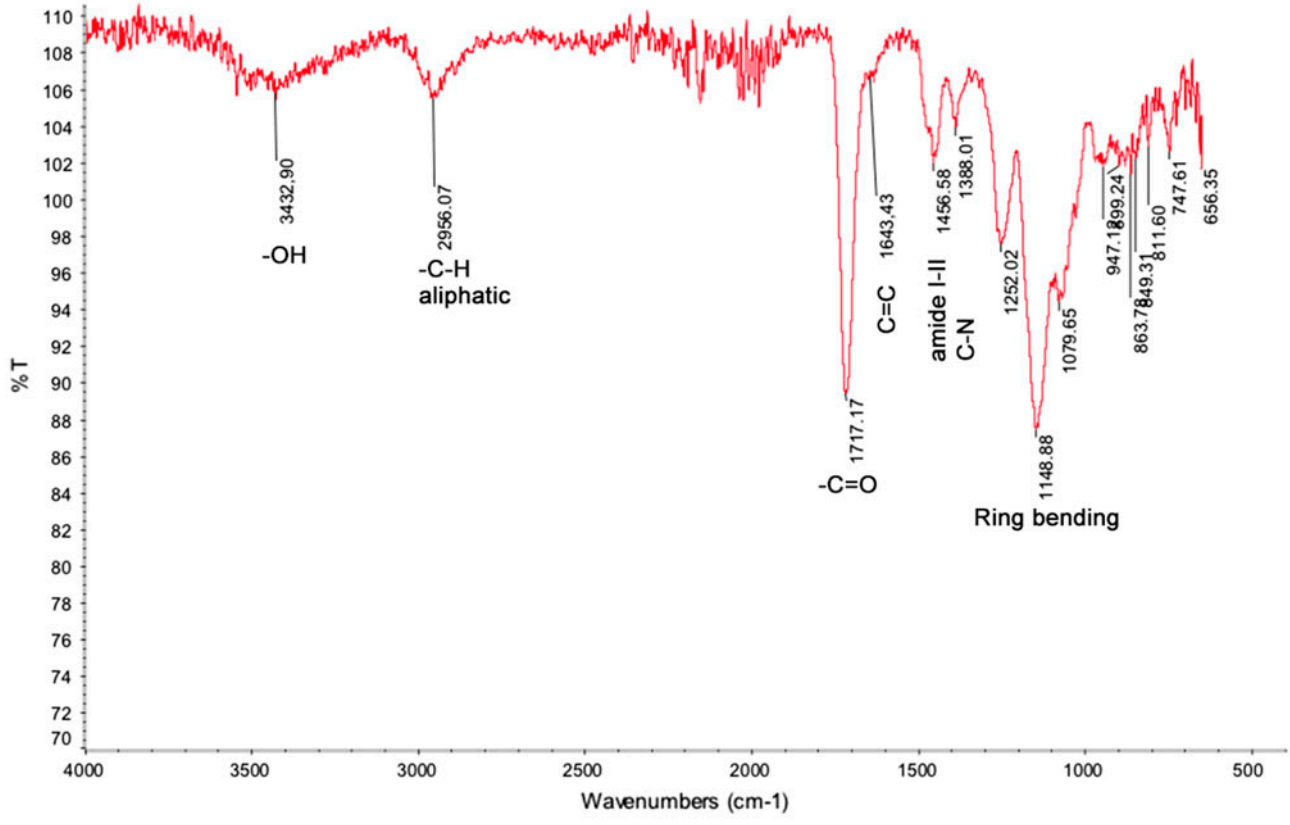

Fig. 5. FTIR spectrum of magnetic microparticles.

3.2.2. *Effect of microparticle amount*

For examining the effect of amount of magnetic microparticles in adsorption medium on the degree of adsorption, magnetic microparticles of 5–100 mg were used during adsorption process at pH 4.0 (Fig. 7). As seen from the figure, adsorption capacity was increased primarily with increasing amount of microparticles, which increases the number of binding sites for VBR. Then, especially after adding microparticles of 50 mg, adsorption capacity did not change

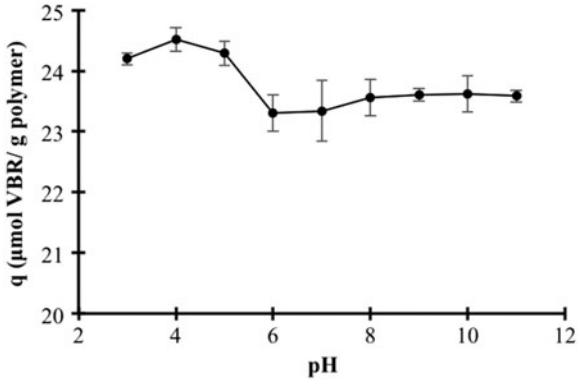

Fig. 6. Effect of solution pH on VBR adsorption. C_{VBR}: 20 mg/L; interaction time: 60 min; microparticle amount: 50 mg; temperature: 25°C.

significantly. As a result of experiments, it is decided that adsorption capacity was fixed at microparticles amount of 50 mg, and thus later, studies were conducted considering the result obtained.

3.2.3. Effect of interaction time

Adsorption process was conducted at the adsorption time of 5–120 min at optimum pH value and adsorbent amount determined. Adsorption capacity values calculated during that time intervals were given at Fig. 8. As seen from the figure, adsorption of VBR at magnetic microparticles was taken place in relatively short time. Ninety-eight percent of the maximum adsorption capacity was achieved at the first 10 min of interaction. After 60 min, the adsorption capacity did not change significantly because of saturation of active binding site and establishing dynamic equilibrium between solid and liquid phases. Therefore, the optimal contact time of 60 min was designated and applied in all studies.

3.2.4. Effect of temperature

To examine the effect of temperature on the adsorption, adsorption process was conducted at 4, 22, 30, 40, 50, and 60°C. As a result of the experiments, it has been noticed that the amount of adsorption was increased with increasing temperature (Fig. 9).

As noted previously, a tryptophan-based monomer was used as a functional monomer. Thus, the principle interactions between the analyte (VBR) and ligand (MATrp) were expected to have hydrophobic character. Results obtained were confirmed these expectations as the increasing adsorption capacity with increasing temperature due to the fact that hydrophobic interactions are directly proportional to temperature.

3.2.5. Effect of ionic strength

To investigate the effect of ionic strength on adsorption capacity, NaCl and $(NH_4)_2SO_4$ salts were studied. Adsorption process was conducted separately with the solution having 10–400 mM salt concentration, and then adsorption capacities of these solutions were calculated after adsorption process completed. As expected, capacity of adsorption was increased with increasing ionic strength (Fig. 10). According to this result, it could be said that analyte–ligand interactions are based on hydrophobicity. Because the presence of salt disturbs the distribution of water around the apolar (hydrophobic) group and provides more

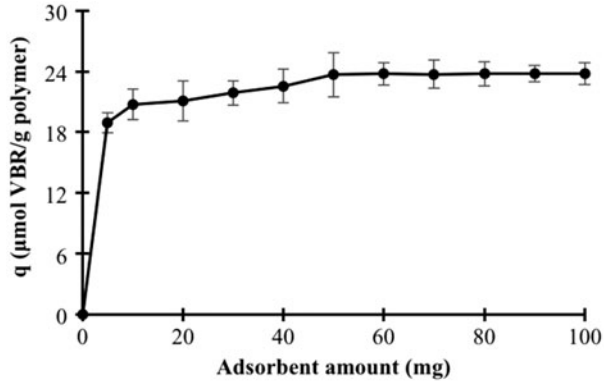

Fig. 7. Effect of adsorbent amount on VBR adsorption. pH 4.0; C_{VBR}: 20 mg/L; interaction time: 60 min; temperature: 25°C.

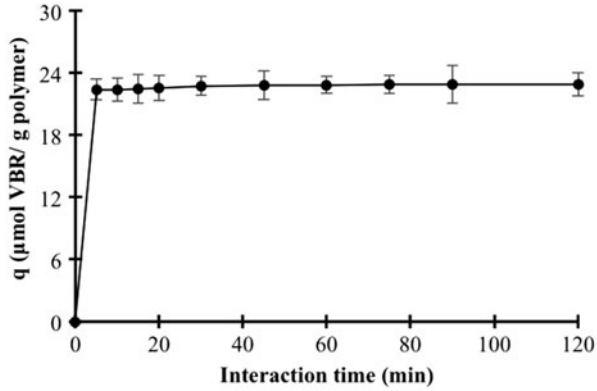

Fig. 8. Effect of interaction time on VBR adsorption, pH 4.0; C_{VBR}: 20 mg/L; microparticle amount: 50 mg; temperature: 25°C.

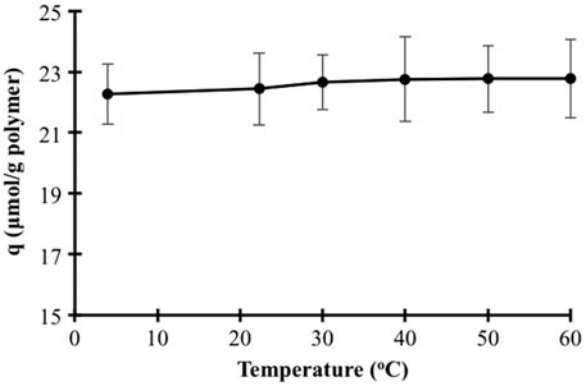

Fig. 9. Effect of ambient temperature on VBR adsorption. pH 4.0; C_{VBR}: 20 mg/L; interaction time: 60 min; microparticle amount: 50 mg.

accessibility to apolar groups. Thus, the presence of salt increases the likelihood of apolar–apolar interaction and a higher adsorption capacity could be achieved.

3.2.6. Comparison of VBR adsorption capacities of plain and hydrophobic microparticles

VBR adsorption onto plain [poly(HEMA)] and hydrophobic [m-poly(HEMA-MATrp)] microparticles was studied with batch system separately (Fig. 11). As seen from the graph, plain microparticles non-specifically adsorbed target VBR because of diffusing into micropores of microparticle and/or interacting with rough surface through physical adsorption. But, by means of incorporation of functional MATrp monomer into the structure, adsorption capacity enhanced significantly due to specific interaction between MATrp groups and VBR molecules. These results proved the appropriateness of MATrp monomer as a functional group for VBR removal in light of the specific analyte–ligand interaction.

3.3. Desorption and reusability

Desorption of VBR dye adsorbed by the magnetic microparticles was studied batchwise as well to show reusability of the adsorbent. Magnetic nanoparticles (0.05 g) adsorbed dye was mixed with 0.5 M HCl solution in 10 mL of desorption media continuously for 1 h. To show the reusability of particles, adsorption–desorption cycle was repeated four times using the same particles. After each adsorption–desorption cycle, the magnetic microparticles were washed with 1.0 M HCl solution for 30 min for sterilization purpose. After this process, microparticles were washed with distilled water for 30 min and then were equilibrated with acetate buffer (pH 4.0) for the next cycle. The result revealed that VBR dye was recovered with the ratio of 99% as a result of adsorption–desorption cycle, and there was no noticeable reduction observed in the adsorption capacity (from 23.87 to 23.52 µmol/g) (Fig. 12).

3.4. Adsorption isotherms

To characterize the relationship between VBR dye and magnetic microparticles, adsorption isotherms were calculated. For this aim, we have evaluated the relationship between initial VBR concentration and dynamic adsorption capacity (Fig. 13(a)) and both

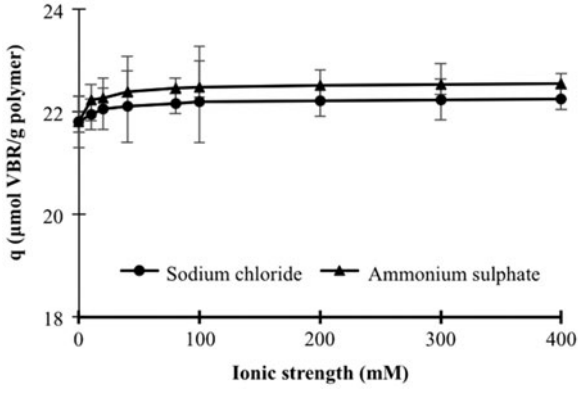

Fig. 10. Effect of ionic strength on VBR adsorption. pH 4.0; C_{VBR}: 20 mg/L; interaction time: 60 min; microparticle amount: 50 mg; temperature: 25°C.

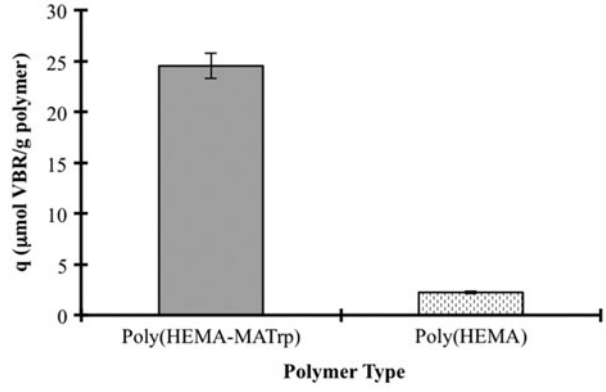

Fig. 11. Comparison of VBR adsorption capacities of plain and hydrophobic microparticles. pH 4.0; C_{VBR}: 20 mg/L; interaction time: 60 min; microparticle amount: 50 mg; temperature: 25°C.

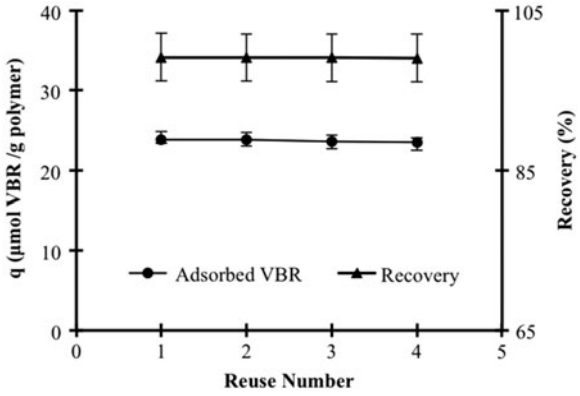

Fig. 12. Reusability of microparticles. pH 4.0; C_{VBR}: 20 mg/L; interaction time: 60 min; microparticle amount: 50 mg; temperature: 25°C.

commonly used isotherms, Langmuir and Freundlich were applied on the experimental data. According to Langmuir adsorption isotherm, the adsorption is considered to be happen at the surface homogeneous and as a single layer, whereas Freundlich isotherm indicates the adsorption process as being not limited at monolayer and considers the adsorption to be heterogeneous. For Langmuir and Freundlich isotherms, following equations were used:

$$\text{Langmuir equation: } Q_{eq} = Q_{max} \cdot b \cdot C_{eq}/(1 + b \cdot Q_{max}) \quad (2)$$

As a result of linearization of this equation:

$$1/Q_{eq} = [1/(Q_{max} \cdot b)](1/C_{eq}) + [1/Q_{max}] \quad (3)$$

From the $1/C_{eq}$ vs. $1/Q_{eq}$ plot, $1/Q_{max}$ and $1/Q_{max} \cdot b$ values can be obtained using y-intercept and slope of the curve, respectively (Fig. 13(b)). Wherein Q is the amount of dye adsorbed (µmol/g), C_{eq} is the amount of dye at equilibrium, b is the Langmuir adsorption constant (L/µmol), and Q_{max} is maximum capacity (µmol/g).

$$\text{Freundlich equation: } \ln Q_{eq} = \ln K_F + (1/n \times \ln C_{eq}) \quad (4)$$

Here, K_F and n indicate Freundlich adsorption isotherm the constant. From the $\ln Q_{eq}$ vs. $\ln C_{eq}$ plot, $\ln K_F$ and $1/n$ values can be used to find y-intercept and slope, respectively (Fig. 13(c)).

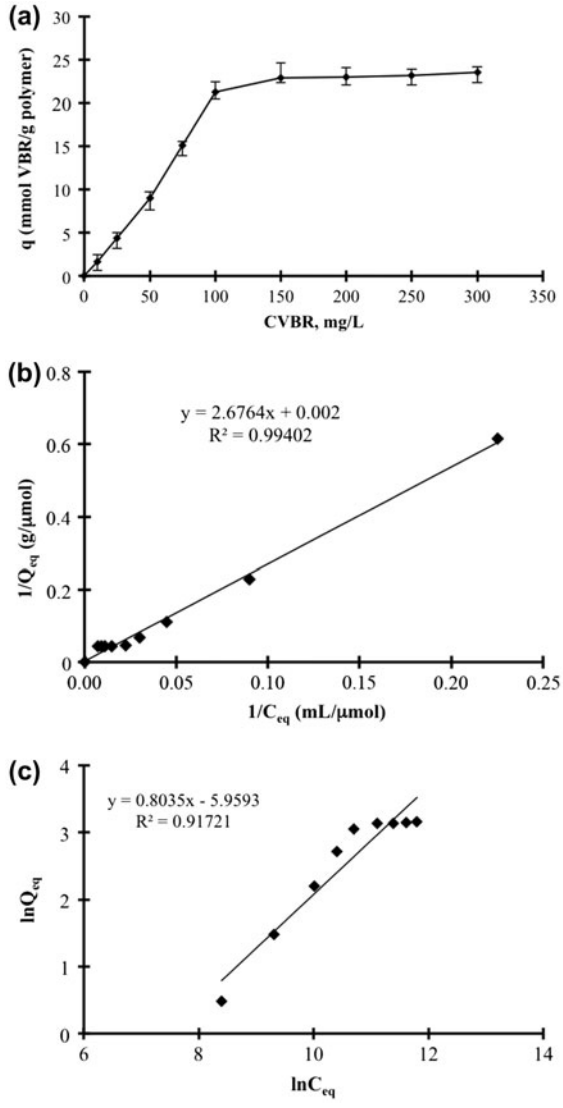

Fig. 13. Adsorption isotherms calculated for VBR adsorption. (a) The relationship between initial VBR concentration and adsorption capacity, (b) Langmuir isotherm and (c) Freundlich isotherm for VBR adsorption.

Adsorption and correlation constants required for both adsorption isotherms were calculated and shown by Table 1. According to the experimental data obtained, correlation coefficient of Langmuir isotherm was higher and Q_{max} value was compatible with the actual data obtained in the experiments. So, the adsorption process was homogeneously on the surface of the microparticles. Adsorption occurred in all regions was energetically equivalent, and lateral interactions between neighboring regions were limited or not available.

Table 1
Parameters calculated from adsorption isotherms

	Langmuir constants			Freundlich constants		
$Q_{experimental}$ (μmol/g)	Q_{max} (μmol/g)	b (mL/μmol)	R^2	K_F ($\times 10^{-3}$)	$1/n$	R^2
89.46	500.0	0.747	0.99402	2.582	0.8035	0.91721

3.5. Adsorption kinetic modeling

Kinetic model estimation was performed as pseudo-first order and pseudo-second order. The linear form of pseudo-first-order equation is as given below:

$$\log [q_{eq} - q_t] = \log (q_{eq}) - (k_1 \cdot t)/2.303 \quad (5)$$

In this equation, k_1 is the pseudo-first-order rate constant of adsorption (1/min) and q_{eq} and q_t are the amount of dye (μmol/g) at balance and adsorbed at time t, respectively. According to this kinetic model, log (q_{eq}) vs. t should give a linear graph (Fig. 14(a)).

The linear form of pseudo-second-order differential equation is given as below:

$$(t/q_t) = (1/k_2 \cdot q_{eq}^2) + (1/q_{eq})t \quad (6)$$

In this equation, k_2 is the pseudo-second-order adsorption rate constant (g/μmol min) and q_{eq} and q_t are the amount of dye at balance and adsorbed at time t (μmol/g), respectively. According to this kinetic model, t/q_t vs. t should give a linear graph (Fig. 14(b)).

The data obtained for both models were summarized in Table 2. According to the results, it could be concluded that q_{eq} value obtained from the pseudo-second-order model was very close to the experimental q_{eq} value and the correlation coefficient was quite high. So, dye adsorption on the magnetic microparticles was fit to second-order kinetic model. As a result, the adsorption process of VBR dye onto magnetic microparticles was chemisorption and controlled by chemical interactions between MATrp groups and VBR molecules without any diffusional restrictions.

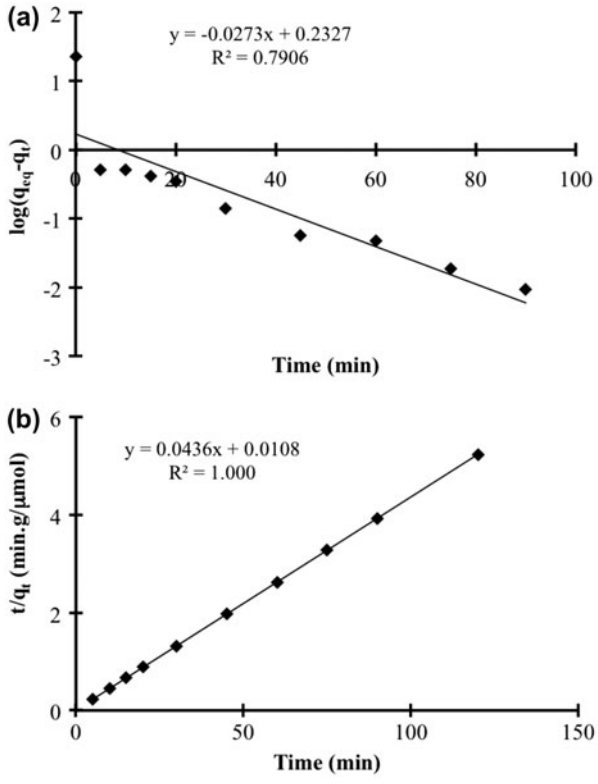

Fig. 14. (a) Pseudo-first-order and (b) pseudo-second-order kinetic models calculated for experimental data.

Table 2
Parameters calculated from kinetic models

	Pseudo-first-order equation: $y = -0.0273x + 0.2327$			Pseudo-second-order equation: $y = 0.0436x + 0.0108$		
$Q_{experimental}$ (μmol/g)	q_{eq} (μmol/g)	k_1 (1/min)	R^2	q_{eq} (μmol/g)	k_2 (g/μmol min)	R^2
22.89	1.709	0.0629	0.7906	22.936	0.176	1.0000

4. Conclusions

It is determined that the magnetic microparticles were quite suitable for the adsorption of VBR dye from aqueous solutions. It was thought that interaction was taken place between hydrophobic indole rings of tryptophan molecules located on the surface of the microparticles and hydrophobic benzene and alkyl groups of dye. Increasing in adsorption amount with the increasing adsorption temperature and ionic strength was an indication of the hydrophobic interactions as well. Interaction between microparticles and dye molecules was well fitted to the Langmuir adsorption model, i.e. the dye molecules were adsorbed on a fixed number of well-defined regions, each of which held only single molecule. Moreover, these regions were equal in terms of energy, and thus, there was no interaction assumed between the adsorbed molecules and available neighboring (adjacent) regions.

Acknowledgments

This study was supported by Hacettepe University, Scientific Research Projects Coordination Unit with a grant number as 013 D10 601 003. L. Uzun thanks to Prof. A. Denizli from Hacettepe University, Ankara, Turkey for his valuable contributions and supporting facilities.

References

[1] M.A. Fox, M.T. Dulay, Heterogeneous photocatalysis, Chem. Rev. 93 (1993) 381–433.
[2] T. Gessner, U. Mayer, Triarylmethane and diarylmethane dyes, in: F. Ullmann, M. Bohnet (Eds.), Ullmann's Encyclopedia of Industrial Chemistry, vol. 37, Wiley-VCH, Weinheim, 2012, pp. 425–478.
[3] W. Azmi, R.K. Sani, U.C. Banerjee, Biodegradation of triphenylmethane dyes, Enzyme Microb. Technol. 22 (1998) 185–191.
[4] D.M. Marmion, Handbook of U.S. Colorants: Food, Drugs, Cosmetics and Medical Devices, third ed., Wiley, New York, NY, 1991.
[5] M.S. Baptista, G.L. Indig, Effect of BSA binding on photophysical and photochemical properties of triarylmethane dyes, J. Phys. Chem. B 102 (1998) 4678–4688.
[6] O. Demirbaş, M. Alkan, M. Doğan, The removal of victoria blue from aqueoussolution by adsorption on a low-cost material, Adsorption 8 (2002) 341–349.
[7] S. Qadri, A. Ganoe, Y. Haik, Removal and recovery of acridine orange from solutions by use of magnetic nanoparticles, J. Hazard. Mater. 169 (2009) 318–323.
[8] G. Mezohegyi, A. Kolodkin, U.I. Castro, C. Bengoa, F. Stuber, J. Font, A. Fabregat, A. Fortuny, Effective anaerobic decolorization of azo dye acid orange 7 in continuous upflow packed-bed reactor using biological activated carbon system, Ind. Eng. Chem. Res. 46 (2007) 6788–6792.
[9] H. Zollinger, Color Chemistry, third ed., Verlag Helvetica Chimica Acta AG, Zurich, 2003.
[10] N. Dizge, C. Aydiner, E. Demirbas, M. Kobya, Adsorption of reactive dyes from aqueous solutions by fly ash: Kinetic and equilibrium studies, J. Hazard. Mater. 150 (2008) 737–746.
[11] K.T. Chen, C.S. Lu, T.H. Chang, Y.Y. Lai, T.H. Chang, Comparison of photodegradative efficiencies and mechanisms of Victoria Blue R assisted by nafion-coated and fluorinated TiO_2 photocatalysts, J. Hazard. Mater. 174 (2010) 598–609.
[12] I. Koyuncu, D. Topacik, E. Yuksel, Reuse of reactive dyehouse wastewater by nanofiltration: Process water quality and economical implications, Sep. Purif. Technol. 36 (2004) 77–85.
[13] B.H. Tan, T.T. Teng, A.K.M. Mohd Omar, Removal of dyes and industrial dye wastes by magnesium chloride, Water Res. 34 (2000) 597–601.
[14] J. Sarma, A. Sarma, K.G. Bhattacharyya, Biosorption of commercial dyes on *Azadirachta indica* leaf powder: A case study with a basic dye rhodamine B, Ind. Eng. Chem. Res. 47 (2008) 5433–5440.
[15] B. Edip, A. Erol, Electrochemically enhanced removal of polycyclic aromatic basic dyes from dilute aqueous solutions by activated carbon cloth electrodes, Environ. Sci. Technol. 44 (2010) 6331–6336.
[16] D.H. Hatchinson, C.W. Robinson, A microbial regeneration process for granular activated carbon—II, Regen. Stud., Water Res. 24 (1990) 1217–1223.
[17] Y. Xu, C.H. Langford, UV- or visible-light-induced degradation of X3B on TiO_2 nanoparticles: The influence of adsorption, Langmuir 17 (2001) 897–902.
[18] R.D. Ambashta, M. Sillanpää, Water purification using magnetic assistance: A review, J. Hazard. Mater. 180 (2010) 38–49.
[19] M. Cerff, M. Morweiser, R. Dillschneider, A. Michel, K. Menzel, C. Posten, Harvesting fresh water and marine algae by magnetic separation: Screening of separation parameters and high gradient magnetic filtration, Bioresour. Technol. 118 (2012) 289–295.
[20] J.K. Lim, D.C.J. Chieh, S.A. Jalak, P.Y. Toh, N.H.M. Yasin, B.W. Ng, A.L. Ahmad, Rapid magnetophoretic separation of microalgae, Small 8 (2012) 1683–1692.
[21] I. Safarik, K. Pospiskova, K. Horska, M. Safarikova, Potential of magnetically responsive (nano)biocomposites, Soft Matter 8 (2012) 5407–5413.
[22] C.H. Yu, K.Y. Tam, C.C.H. Lo, S.C. Tsang, Functionalized silica coated magnetic nanoparticles with biological species for magnetic separation, IEEE Trans. Magn. 43 (2007) 2436–2438.
[23] C.J. Chen, Y. Haik, J. Chatterjee, Size dependent magnetic properties of iron oxide nanoparticles, J. Magn. Magn. Mater. 257 (2003) 113–118.
[24] Y. Haik, J. Chatterjee, C.J. Chen, Synthesis and stabilization of Fe–Nd–B nanoparticles for biomedical applications, J. Nanopart. Res. 7 (2005) 675–679.
[25] R. Sharma, Y. Haik, C.J. Chen, Superparamagnetic iron oxide-myoglobin as potential nanoparticle: Iron

oxide-myoglobin binding properties and magnetic resonance imaging marker in mouse imaging, J. Exp. Nanosci. 2 (2007) 127–138.
[26] T. Lund-Olesen, H. Bruus, M.F. Hansen, Quantitative characterization of magnetic separators: Comparison of systems with and without integrated microfluidic mixers, Biomed. Microdevices 9 (2007) 195–205.
[27] I. Safarik, M. Safarikova, Magnetic nano- and microparticles in biotechnology, Chem. Pap. 63 (2009) 497–505.
[28] M. Safarikova, B.M.R. Pona, E. Mosiniewicz-Szablewska, F. Weyda, I. Safarik, Dye adsorption on magnetically modified *Chlorella vulgaris* cells, Fresenius Environ. Bull. 17 (2008) 486–492.
[29] G. Prochazkova, I. Safarik, T. Branyik, Surface modification of Chlorella vulgaris cells using magnetite particles, Proc. Eng. 42 (2012) 1951–1961.
[30] L. Xu, C. Guo, F. Wang, S. Zheng, C.Z. Liu, A simple and rapid harvesting method for microalgae by in situ magnetic separation, Bioresour. Technol. 102 (2011) 10047–10051.
[31] C.T. Yavuz, A. Prakash, J.T. Mayo, V.L. Colvin, Magnetic separations: From steel plants to biotechnology, Chem. Eng. Sci. 64 (2009) 2510–2521.
[32] F. Yılmaz, N. Bereli, H. Yavuz, A. Denizli, Supermacroporous hydrophobic affinity cryogels for protein chromatography, Biochem. Eng. J. 43 (2009) 272–279.